

Heparin binding sites on Ross River virus revealed by electron cryo-microscopy

Wei Zhang, Marintha Heil¹, Richard J. Kuhn, Timothy S. Baker^{*,2}

Department of Biological Sciences, Purdue University, West Lafayette, IN 47907-2054, USA

Received 30 August 2004; returned to author for revision 20 September 2004; accepted 29 November 2004

Available online 8 January 2005

Abstract

Cell surface glycosaminoglycans play important roles in cell adhesion and viral entry. Laboratory strains of two alphaviruses, Sindbis and Semliki Forest virus, have been shown to utilize heparan sulfate as an attachment receptor, whereas Ross River virus (RRV) does not significantly interact with it. However, a single amino acid substitution at residue 218 in the RRV E2 glycoprotein adapts the virus to heparan sulfate binding and expands the host range of the virus into chicken embryo fibroblasts. Structures of the RRV mutant, E2 N218R, and its complex with heparin were determined through the use of electron cryo-microscopy and image reconstruction methods. Heparin was found to bind at the distal end of the RRV spikes, in a region of the E2 glycoprotein that has been previously implicated in cell-receptor recognition and antibody binding.

© 2004 Published by Elsevier Inc.

Keywords: Alphavirus; Ross River virus; Heparan sulfate; Heparin; Electron cryo-microscopy; GAG; Three-dimensional reconstruction

Introduction

Alphaviruses comprise a genus (*Togaviridae* family) of 26 viruses that are transmitted by arthropods and contain a plus sense RNA genome (Strauss and Strauss, 1994). They include Ross River virus (RRV), Semliki Forest virus (SFV), Sindbis virus (SINV), and Aura virus. Alphaviruses replicate in a diverse range of vertebrate and invertebrate animals as well as a wide variety of cultured cells. Such a broad host range suggests that alphaviruses may employ a ubiquitous cellular receptor to enter cells, or they may use different sets of receptors for different host cells (Strauss et al., 1994). In addition to several putative protein receptors described for SINV, heparan sulfate (HS), a cell surface

glycosaminoglycan (GAG), has been implicated as important for alphavirus cellular attachment, though it is not absolutely required for infection (Byrnes and Griffin, 1998). Laboratory strains of SINV (McKnight et al., 1996) display a higher affinity for HS than field isolates (Taylor et al., 1955) and passage of field isolates results in adaptive changes that increase the ability of the virus to utilize HS binding (Klimstra et al., 1998).

HS is a heterogeneously sulfated, negatively charged GAG that consists of repeating disaccharide units of L-iduronic acid and D-glucosamine joined by an α (1–4) linkage. HS is implicated in cell adhesion and has been shown to serve as an attachment receptor for several viruses such as foot-and-mouth disease virus (FMDV) (Jackson et al., 1996), human immunodeficiency virus type 1 (Patel et al., 1993), dengue virus (Chen et al., 1997), respiratory syncytial virus (Krusat and Streckert, 1997), vaccinia virus (Lin et al., 2000), herpes simplex virus type 1 (WuDunn and Spear, 1989), and adeno-associated virus type 2 (Summerford and Samulski, 1998). The atomic structure of FMDV subtype O₁ complexed with heparin revealed for the first time the detailed molecular interface between heparin and a

* Corresponding author. Fax: +1 858 534 0202.

E-mail address: tsb@chem.ucsd.edu (T.S. Baker).

¹ Present address: Department of Microbiology, The University of Alabama at Birmingham, Birmingham, AL 35294-2170, USA.

² Present address: Department of Chemistry and Biochemistry, University of California at San Diego, 9500 Gilman Drive #0378, La Jolla, CA 92093-0378, USA.

viral protein (Fry et al., 1999). The anionic sulfate group in the bound heparin molecule primarily interacts with the positively charged Arg56 of VP3 and also interacts with Arg135 of VP2. Except for the side chain of His195 of VP1, heparin binding to FMDV did not cause major conformational changes in the viral proteins (Fry et al., 1999).

Tissue culture adapted strains of SINV (Klimstra et al., 1998), Venezuelan equine encephalitis virus (Bernard et al., 2000), and a mutant of RRV (Heil et al., 2001) are known to bind heparin. A single amino acid substitution (Asn to Arg) in the RRV E2 glycoprotein at residue 218 produces virus (RRV E2-N218R; hereafter referred to simply as RRV₂₁₈) that exhibits enhanced HS interaction and an expanded host range for RRV, allowing it to replicate more efficiently in chicken embryo fibroblast cells (Heil et al., 2001). Based on knowledge of the structure RRV and other alphaviruses (Cheng et al., 1995; Mancini et al., 2000; Paredes et al., 1993; Smith et al., 1995), it was postulated that HS would bind to E2 at or near residue 218 at the surface of RRV.

The structures of several alphaviruses have been studied using a combination of electron cryo-microscopy (cryo-EM), three-dimensional (3D) image reconstruction, and molecular modeling (Cheng et al., 1995; Mancini et al.,

2000; Paredes et al., 1993; Pletnev et al., 2001; Zhang et al., 2002a, 2002b). Mature virions are 700 Å diameter, spherical particles composed of two concentric protein layers and an intervening lipid membrane. Viral proteins in both layers are arranged with $T = 4$ icosahedral symmetry (Caspar and Klug, 1962). The nucleocapsid core consists of 240 copies of the 30 kDa nucleocapsid protein (NCP) (Cheng et al., 1995; Choi et al., 1991), which encapsidate the 11.7 kb viral genome. The core is enveloped by a lipid bilayer and an outer shell consisting of two surface glycoproteins, E1 and E2, each of which is anchored in the bilayer with a transmembrane segment. E1 and E2 form stable heterodimers that associate as trimers, giving rise to the 80 prominent spikes that project radially outward from the virus surface (Fig. 1A). The 52 kDa E1 contains the fusion peptide and is responsible for host membrane penetration (Garoff et al., 1980; Strauss and Strauss, 1994). E2 (50 kDa) is involved with receptor interaction and cell recognition (Strauss and Strauss, 1994; Strauss et al., 1991). In an earlier study, the atomic structure of the homologous SFV E1 was fitted into an 11 Å SINV density map and demonstrated that E1 comprises the bulk of the base of the glycoprotein spikes and forms an icosahedral scaffold (Lescar et al., 2001;

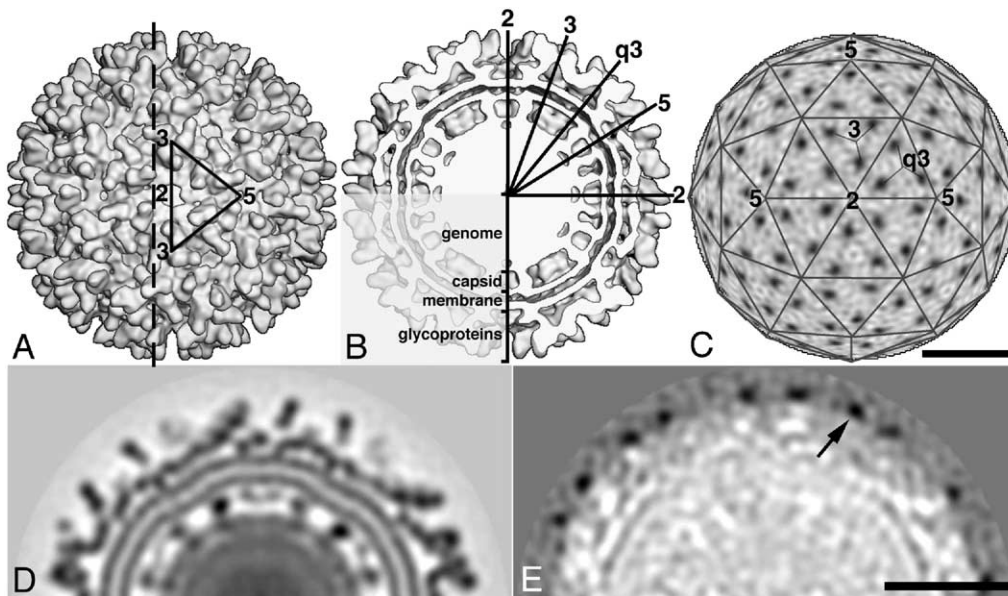


Fig. 1. Cryo-EM reconstructions of RRV₂₁₈ and RRV₂₁₈/HS complex. (A) Shaded-surface representation of RRV₂₁₈ mutant reconstruction map at 22 Å resolution, viewed along a two-fold axis. The open triangle highlights one asymmetric unit of the icosahedral structure, which is defined by the locations of the icosahedral two-, three-, and five-fold axes. The vertical dashed line identifies the position of a plane, 50 Å away from a central (equatorial) plane, corresponding to the density map sections shown in D and E. (B) Same as A but with the closest half computationally removed to expose internal features in the RRV₂₁₈ reconstruction. Some axes of strict (2, 3, and 5) and quasi (q3) symmetry that lie in the central equatorial plane are identified. The lower-left quadrant highlights the approximate radial locations (tick marks along the vertical line) of the different viral components. These regions include the genome ($r < 164$ Å), the capsid (164 Å $< r < 200$ Å), the membrane bilayer (200 Å $< r < 257$ Å), and the glycoprotein shell (257 Å $< r < 353$ Å). (C) Hemispherical density projection ($r = 254$ Å) of the RRV₂₁₈/HS minus RRV₂₁₈ difference map (highest density features appear black). The triangulation net helps illustrate the presence of $T = 4$ quasi-symmetry and identifies virtual boundaries that separate the 80 trimeric glycoprotein spikes, twenty of which occur at the strict three-fold axes and the remaining sixty of which occur at the quasi-three-fold positions. The punctate black dots correspond to the bound heparin molecules. About half of the 240 total heparin molecules are depicted in this hemisphere projection. Scale bar represents 200 Å for panels A–C. (D) Non-equatorial cross-section from the RRV₂₁₈ reconstruction, extracted from the portion of the density map highlighted by the dashed line in A. This 1-pixel thick, density projection provides a slightly magnified, alternative view of the internal, multilayered RRV structure comparable to that shown in the top half of panel B. (E) Same as D but from the RRV₂₁₈/HS minus RRV₂₁₈ difference map. The most prominent and darkest features (arrow) all occur at a radius centered at 254 Å and are attributable to the presence of heparin molecules in the complex. Scale bar represents 200 Å for panels D and E.

Zhang et al., 2002b). E2 interacts extensively with E1 to form a heterodimer and the C-terminal tail of E2 binds to the NCP (Lee et al., 1996; Strauss and Strauss, 1994). To date, no atomic structure of an alphavirus E2 glycoprotein has been determined. Consequently, current knowledge of E2 structure is primarily deduced from analysis of a difference density map computed between the 11-Å SINV reconstruction and a model based on the fitted E1 atomic structure (Zhang et al., 2002b). This difference map shows E2 to be an elongated molecule that is similar in size and shape to E1 and comprises both the center and highest radius portions of the trimeric spikes.

The locations of the N-linked glycosylation sites in glycoproteins E1 and E2 in SINV, Aura, and RRV have been determined (Pletnev et al., 2001; Zhang et al., 2002a). The carbohydrate sites in RRV occur on residue 141 in E1 and on residues 200 and 262 in E2. E1–141 and E2–262 are at low radii (<315 Å), whereas E2–200 is at radius of 348 Å at the distal tip of the spikes, near the binding site of the E2 monoclonal antibody T10C9 that was identified in previous cryo-EM studies (Smith et al., 1995). An escape mutant of this antibody maps to residue 216 of E2 and is therefore just two residues away from the N218R mutation site that confers HS binding to RRV.

Here we present the results of a cryo-EM and 3D image reconstruction study that identifies the site of HS binding to RRV₂₁₈. Image reconstructions of RRV₂₁₈ and RRV₂₁₈ complexed with HS were computed to 22- and 24-Å resolution, respectively. A difference map between the RRV₂₁₈/HS complex and RRV₂₁₈ revealed the presence of 240 ellipsoidal masses that we attributed to the presence of heparin in the complexes. The bound heparin molecules occupy sites at the distal surface of the glycoprotein spikes in regions corresponding to the E2 densities. The heparin binding footprint overlaps that of the E2 monoclonal antibody T10C9 Fab fragment (Smith et al., 1995). Knowledge of the location of residue 218 provides an additional landmark on E2 that can help further characterize both the structure and function of this viral glycoprotein. The overlapping footprints of the T10C9 antibody and a cell attachment molecule demonstrate a functional overlap of selected amino acid residues on the viral surface and suggest that T10C9 directly inhibits virus binding to the cell surface.

Results and discussion

Heparin binds to the distal tip of the E2 glycoprotein

A 3D reconstruction of the RRV₂₁₈ mutant, reliable to 22 Å resolution, was computed from 1007 virus images selected from nine separate micrographs (Table 1). The outer surface of the RRV₂₁₈ structure (Fig. 1A) is dominated by 80 trimeric glycoprotein spikes that are characteristic of all other alphavirus structures (Cheng et al., 1995; Mancini et al., 2000; Paredes et al., 2003; Zhang et al., 2002a;

2002b). Cross-sectional views of the reconstruction reveal a multilayered structure comprised of genome, nucleocapsid, membrane, and glycoproteins (Fig. 1B). Comparison of the RRV₂₁₈ reconstruction with the 22 Å resolution reconstruction of wild type RRV (Zhang et al., 2002a) did not reveal any significant structural differences.

A 3D reconstruction at 24 Å resolution of the RRV₂₁₈/HS complex was computed from 706 individual particle images extracted from thirteen micrographs (Table 1). Though images of vitrified samples containing the RRV₂₁₈/HS complex appear slightly noisier than those of the RRV₂₁₈ mutant virus alone, presumably due to a high background concentration of unbound heparin molecules, a difference map between the RRV₂₁₈/HS complex and RRV₂₁₈ alone clearly depicted 240 strong density features attributable to bound heparin molecules (Fig. 1E). Indeed, the magnitudes of these prominent difference density features measured at least three times larger than any other positive or negative features throughout the difference map (Figs. 1C–E). Four independent density peaks occur within each asymmetric unit of the icosahedral structure and their arrangement obeys $T = 4$ quasi icosahedral symmetry (Fig. 1C) (Pletnev et al., 2001). The centers of the difference density peaks are all located at a radius of 375 Å, which corresponds to the distal ends of the glycoprotein spike petals. In addition, all of these peaks lie at positions that are ~54 Å away from the spike axis.

Heparin molecules are known to be long, flexible, and heterogeneous (Fry et al., 1999). Consequently, heparin is not expected to adopt a unique conformation or structure, and the density we attribute to it in our image reconstruction must therefore represent an average of multiple possible structures. Even so, the four unique heparin densities within each asymmetric unit exhibit a similar ellipsoid shape (~35 Å long and 17 Å diameter) (Fig. 2). The heparin used in this study contains an average of about 10 disaccharide repeat units with a total mass of ~6 kDa. We estimate that each heparin density in the RRV–heparin complex corresponds to about four repeat units. This estimate is based upon reference to the X-ray crystallographic structure of FMDV complexed with its heparin receptor (Fry et al., 1999), in which two-and-one-half heparin repeat units (5 sugar molecules) occupies a length of 21 Å.

The sole loss of a positively charged arginine residue at E2 position 218 renders native RRV incapable of binding heparin. Consequently, heparin binding to the RRV₂₁₈

Table 1
Data collection and image processing statistics

| Reconstruction | M | Defocus (μm) | P (# used) | Resolution (Å) |
|------------------------|----|--------------|-------------|----------------|
| RRV ₂₁₈ | 9 | 1.42–2.41 | 1651 (1007) | 22 |
| RRV ₂₁₈ /HS | 13 | 1.88–2.48 | 1030 (706) | 24 |

M, number of micrographs; Defocus, range of defocus settings for set of micrographs; P = total number of particle images selected from micrographs; # used, number of particle images included in three-dimensional reconstruction.

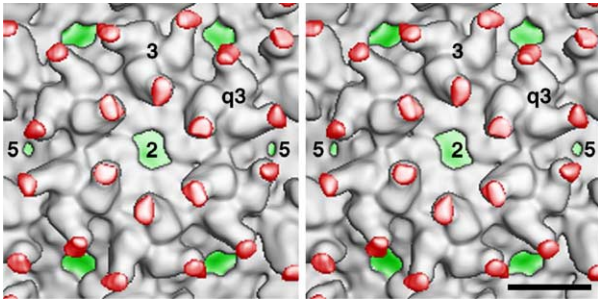


Fig. 2. Shaded-surface stereo view of a portion of the RRV₂₁₈/HS reconstruction with the difference map (red) superimposed to highlight the locations of the heparin molecules at the tips of the trimeric spikes. The viral membrane (green) is visible through the large holes at the icosahedral two-fold axes (central one is labeled “2”) and also through the smaller holes at the five-fold (two are labeled “5”). Scale bar is 100 Å.

mutant is primarily attributed to electrostatic interactions between the negatively charged sulfate groups of heparin and the positively charged arginine and possibly other nearby basic residues. Two lysine residues at positions 215 and 221 are close in sequence to R218 of E2, and though they are insufficient on their own to support productive binding of heparin, they appear to be likely candidates to enhance the association between RRV₂₁₈ and heparin.

Though the expansion of the host range for the mutant RRV₂₁₈ is a consequence of the newly acquired virion–HS interaction, it may be that HS only functions as a co-receptor, which acts to draw virions to the cell surface where they are then able to interact with another or other receptors. Association with HS therefore enhances the accessibility of the true viral receptor to specific interactions with E2. In fact, within alphaviruses, the sequences of the receptor-binding region in E2 (surrounding residue 218) are not conserved, and mutation of one or more residues in this region can result in a mutant virus that utilizes additional receptors and infects an expanded set of hosts.

Aside from the 240 prominent peaks mentioned above, no other significant differences appear in the difference map. Hence, at least at a resolution of 24 Å, the RRV structure is unaltered by its association with heparin.

The heparin binding footprint overlaps the footprint of monoclonal antibody T10C9

The E2 glycoprotein of alphaviruses interacts with host cells and is the primary determinant for antibody neutralization (Strauss and Strauss, 1994; Smith et al., 1995). Several lines of evidence suggest that the distalmost tip of E2 represents a site for both antibody and receptor binding. First, anti-idiotypic antibodies generated against neutralizing antibody SV209 (anti-ID 209) bound to N18 neuroblastoma cells and reduced virus binding by 50%. Anti-ID 209 led to the identification of a receptor for SINV (Ubol and Griffin, 1991). Second, like SV209, the T10C9 neutralizing antibody to RRV is also believed to recognize an epitope that overlaps or lies adjacent to a receptor interaction site. An epidemic outbreak of RRV in the Pacific islands occurred in 1979–1980. Comparison of the E2 genes from RRV F9073 (Fiji), RRV 213970 (American Samoa), and RRV 215398 (Cook Islands) showed that RRVs 213970 and 215398 have identical sequences whereas F9073 differs by a single amino acid at position 219. Mutation at this position was suggested to result from the recognition of a new host cell receptor (Burness et al., 1988). E2 residue 219 is located close to an epitope on RRV recognized by neutralizing monoclonal antibody T10C9. Escape mutants of T10C9 map to residue 216 of E2 in RRV (Vrati et al., 1988). Cryo-EM reconstructions of wild type RRV and SINV complexed with Fab fragments of antibodies SV209 and T10C9, respectively, demonstrated that antibodies bind to the outermost tips of the trimeric glycoprotein spikes (Smith et al., 1995).

Comparison of the RRV₂₁₈ and RRV₂₁₈/HS reconstructions with those of RRV and SINV to which antibodies had been bound (Smith et al., 1995) clearly demonstrated an overlap between the HS and antibody binding footprints (Fig. 3). The centers of the Fab and heparin footprints lie about 10 Å apart. Indeed, the RRV₂₁₈ mutant is no longer neutralized by monoclonal antibody T10C9 (Heil et al., 2001), indicating that residue E2–218 also affects T10C9 reactivity. Extensive overlap of the footprints of antibodies

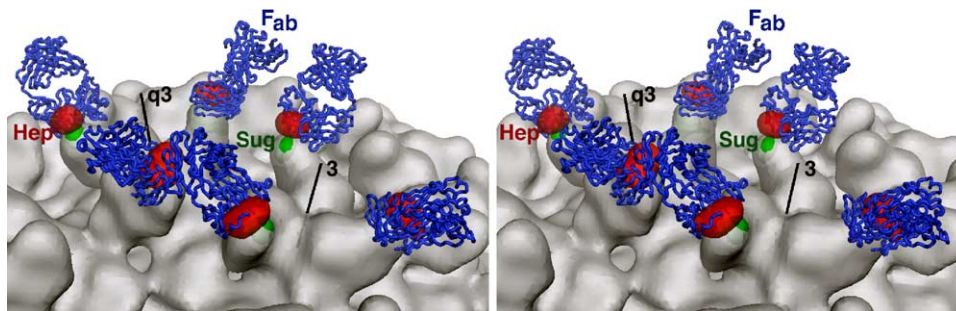


Fig. 3. Stereo view of neighboring three-fold (3) and quasi-three-fold (q3) spikes in the RRV₂₁₈ reconstruction showing the locations of the carbohydrate moieties at residue 200 of the E2 glycoprotein (green dot labeled “Sug”), the difference densities attributed to the heparin molecules (red ellipsoids labeled “Hep”), and Fab molecules (blue atomic model chain traces). The heparin molecules are presumed to bind at E2 residue 218 and the Fabs were earlier shown (Smith et al., 1995) to bind at or near E2 residue 216. The positions of the carbohydrate moieties in RRV were determined on the basis of inspection of a difference map computed between RRV and SINV. The program DINO (<http://www.dino3d.org>) was used to help prepare this figure as well as Fig. 4.

SV209 and T10C9 and heparin supports the hypothesis that the outer portion of the spike tip is a conserved receptor-binding site. Alternatively, additional, non-overlapping regions that recognize cell receptors may be present in alphaviruses.

The carbohydrate moiety at E2 residue 200 in RRV does not appear to mask out either the heparin HS (Heil et al., 2001) or Fab (Smith et al., 1995) binding sites (Fig. 3) since the density attributed to the carbohydrate chain at residue 200 does not overlap the heparin or Fab density. This contrasts with the situation observed for influenza hemagglutinins (HA). In the fowl plague virus HA ectodomain, the N-linked oligosaccharide chains, which lie in close proximity to the neuraminic acid-containing receptor-binding site, appear to control both receptor-binding specificity and affinity (Ohuchi et al., 1997). In addition, glycosylation of HA at antigenic epitopes has been shown to interfere with antibody access to viruses (Skehel et al., 1984). Similar experiments have yet to be performed with alphaviruses.

Residue 196 of the SINV E2 glycoprotein also lies close to the SINV receptor and antibody binding sites (Fig. 4B) (Smith et al., 1995). Loss of the oligosaccharide chain from this site in SINV mutants results in viruses with comparable plaque size but slightly reduced growth rate relative to wild type virus (Pletnev et al., 2001). It is unknown what role if any the carbohydrate chains that lie close to the receptor-binding region in alphaviruses have.

Landmarks on the E2 glycoprotein

No atomic structure of an alphavirus E2 glycoprotein has been determined. Hence, current knowledge about E2 structure is limited to analysis of a difference map, computed by taking an 11 Å resolution reconstruction of SINV and subtracting out density corresponding to the fitted SINV E1 atomic structure (Zhang et al., 2002b). Such analysis showed that E2, like E1, has an elongated ectodomain and a C-terminal transmembrane domain.

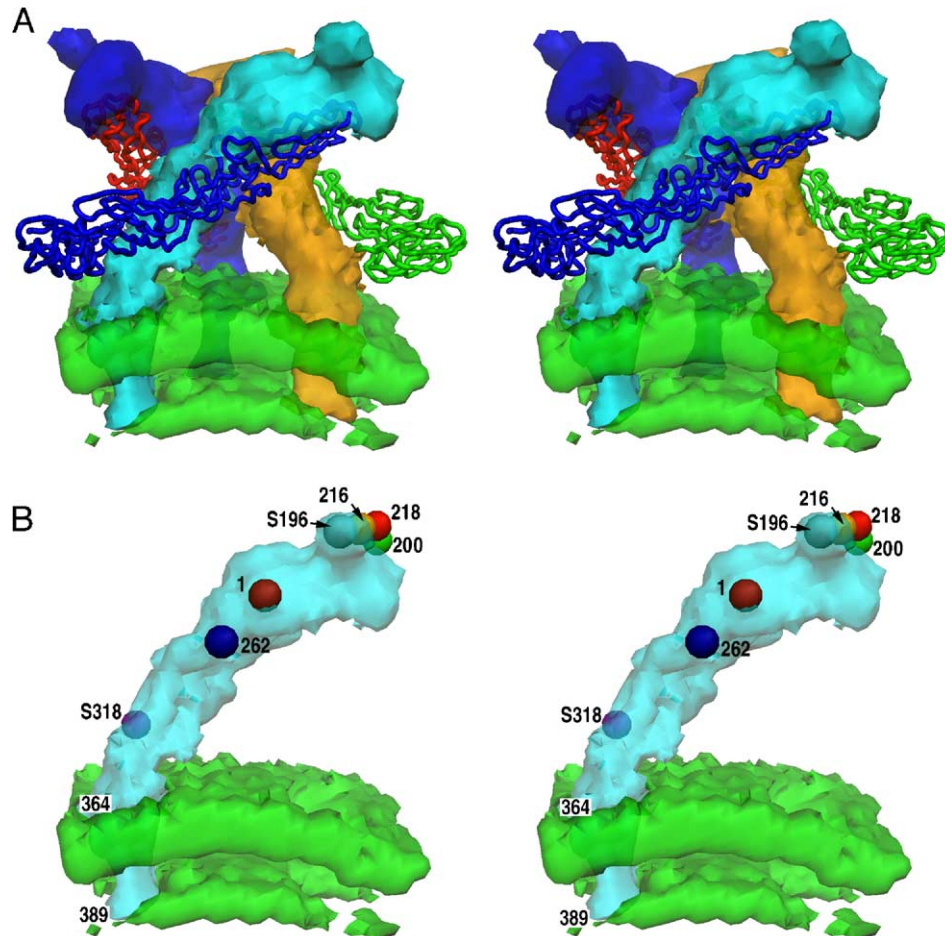


Fig. 4. Landmarks of the E2 glycoprotein. (A) Stereo view of one SINV spike with densities included for three E2 molecules (yellow, blue, and cyan), three homology models of the E1 ectodomain (green, red, and blue polypeptide backbone traces), and the viral bilayer membrane (green). (B) Same as A but with the E1 homology models and two E2 molecules removed to reveal the approximate locations of several residue 'landmarks' (spheres) on a single E2 molecule. RRV residues 200, 216, and 218, and SINV glycosylation site 196 cluster at the high radius tip of E2, ~354-Å from the virus center. The amino terminus of E2 lies near a radius of 325 Å. The approximate locations of RRV residue 262 and SINV glycosylation site 318 (on backside of E2 density) are also depicted. The transmembrane portion of E2 starts and ends at residues 364 and 389, respectively. Not depicted is the carboxy terminal portion of E2 (390–422), which extends beneath the viral membrane toward the nucleocapsid.

Close contacts between the E1 and E2 ectodomains result in the formation of a stable heterodimer. Three of these E1–E2 heterodimers associate to form the characteristic trimeric, clover-leaf-shaped spike (Fig. 4A). The structural roles of E1 and E2 are likely dictated by their locations in the spike. E2 comprises the peripheral surface of the projecting spike and is essential for intra-spike interactions. Though the E1 molecules within a spike do not contact each other, they do contact E1 molecules in adjacent spikes at the base or “skirt” layer and therefore are responsible for inter-spike interactions.

The approximate locations of several E2 residues in the ectodomain have been determined on the basis of analyses of cryo-EM reconstructions from several, closely related alphaviruses (Pletnev et al., 2001; Zhang et al., 2002a) (Fig. 4B). For example, in RRV, the glycosylation site at residue 200, the antibody T10C9 binding site (Smith et al., 1995) at residue 216, and the heparin binding site at residue 218 have all been located within the outermost region of the spike. The second glycosylation site at residue 262 in RRV maps to the central region of the protein ectodomain and lies close to the base of the spike between two neighboring spikes (Pletnev et al., 2001). The two glycosylation sites in the SINV E2 glycoprotein at residues 196 and 318 and in the Aura virus E2 at residues 197 and 319 have also been identified in image reconstructions of these two viruses (Zhang et al., 2002a).

The approximate location of the N-terminus of E2 in alphaviruses was determined in a cryo-EM reconstruction study of a SINV mutant that retains the E3 protein (~10 kDa) (Paredes et al., 1998), which precedes E2 in sequence. Density attributed to E3 in the SINV mutant spans an equivalent region in RRV, along the outer surface of E2 that extends between residues 200 and 262. Furthermore, a number of other studies indicate that E2 residues 55–61 and 232–234 also lie near the N-terminus of E2. E2 residues 232 and 234 are known to be key determinants of the epitope recognized by the RRV-specific monoclonal antibody NB3C4 (Kerr et al., 1993; Vrati et al., 1988). An RRV deletion mutant, in which wild type residues 55–61 are missing, is markedly less reactive with NB3C4 (Vrati et al., 1986), and a point mutation at residue 4 results in virus poorly neutralized by NB3C4 (Kerr et al., 1993). The above results collectively provide strong evidence that the N-terminus of E2 occurs at the approximate location depicted in Fig. 4.

The transmembrane domain of E2 in RRV, which is comprised of residues 364 to 389, is followed by the 33 amino acid, C-terminal tail that lies inside the viral membrane and interacts with the nucleocapsid core (Strauss and Strauss, 1994). The approximate locations of E2 transmembrane fragments in the cryo-EM reconstruction of SINV at 11 Å resolution serve as additional landmarks on the E2 structure (Zhang et al., 2002b).

Until an X-ray structure of an alphavirus E2 protein or fragment becomes available, enhanced knowledge of E2 structure is likely to result from the identification of

additional landmarks combined with higher resolution cryo-EM reconstruction studies of both native and selectively mutated virus samples. If resolution can be improved to sub-nanometer levels (e.g., ~5 Å or better), details of secondary and tertiary structure are more reliably represented and can be interpreted (Kong et al., 2004) and, in conjunction with secondary structure or 3D structure predictions, may lead to plausible models of how E2 functions throughout the viral infection process.

Materials and methods

Viruses and cells

Wild type RRV strain T48 (RR64) and the N218R mutant (RRV₂₁₈) were generated by *in vitro* transcription and transfection into baby hamster kidney (BHK) cells as described (Heil et al., 2001). Both viruses were plaque purified twice on monolayers of BHK cells. Titers of twice passaged stocks were determined based on the average value obtained from three independent plaque assays. These stocks were used as inoculums for virus production. BHK cells were maintained in minimum essential media supplemented with 7.5% fetal bovine serum (FBS), 1× PSN (0.05 mg penicillin per ml, 0.05 mg streptomycin per ml, and 0.1 mg neomycin per ml), 2 mM L-glutamine, and 0.1 mM non-essential amino acids (Life Technologies, Rockville, MD).

Virus purification

For high titer virus stocks, BHK cells were adsorbed with virus at a multiplicity of infection of 0.1 plaque forming unit (pfu)/cell for 1 h at 37 °C. Cells were overlaid with minimum essential media supplemented with 3% FBS, PSN, 2 mM L-glutamine per ml, and 0.1 mM non-essential amino acids. Virus was harvested 20 h post-infection. Supernatants were clarified followed by polyethylene glycol 8000 precipitation (10% PEG and 1 M NaCl) for 6 h at 4 °C. The resulting pellet was resuspended in 2 ml of TNE buffer (0.05 M Tris–HCl [pH7.2], 0.1 M NaCl, and 0.001 M EDTA) and layered on top of a linear 20–60% (wt/vol) sucrose gradient. The gradient was centrifuged for 2 h at 160,000 × *g*. The viral band was collected by extraction with a needle and syringe and concentrated by centrifugation through a 30% sucrose cushion for 1.5 h at 190,000 × *g*. Virus was resuspended in TNE buffer and its titer determined by plaque assay. The measured titers were 3.3 × 10⁹ pfu/ml for native RRV and 1 × 10¹⁰ pfu/ml for RRV₂₁₈.

Virus–heparin complexes

For cryo-EM and image reconstruction, complexes of RRV₂₁₈ and heparin (porcine intestinal mucosa, SIGMA, catalog number H3393) were mixed together at room temperature at a ratio of 1200 molecules of heparin/virion

(approximately 5 heparin molecules per molecule of E2). Before cryo-EM experiments, a small sample of the particles and the particle/heparin complexes were analyzed for aggregation and irregular particle morphology by staining with 2%(w/v) uranyl acetate and visual inspection using a Philips EM420 electron microscope. Samples were placed at 4 °C until frozen for cryo-EM.

Cryo-EM and 3D image reconstruction

Cryo-EM and 3D image reconstruction procedures were carried out essentially as described previously (Baker and Cheng, 1996; Baker et al., 1999; Olson et al., 1990). Images of vitrified samples of RRV₂₁₈ and the RRV₂₁₈/HS complex were recorded in an FEI/Philips CM200 FEG transmission electron microscope under low dose conditions ($\sim 16 \text{ e}^-/\text{\AA}^2$) at a calibrated magnification of 39,200 (Table 1) (Zhang et al., 2003). Micrographs were digitized with a Zeiss-SCAI scanner at 7 μm steps and 2×2 groups of pixels were bin-averaged to yield an effective sampling of 3.57 \AA in the specimen. The parameters that define the view orientation and origin (θ , ϕ , ω , x , and y) of each viral image were determined and refined by means of polar Fourier transform (PFT) procedures (Baker and Cheng, 1996). The interactive graphics routine RobEM (<http://www.bilbo.bio.purdue.edu/~baker/programs/programs.html>) was used to determine the level of defocus in each micrograph. Corrections to partially compensate for the effects of the microscope contrast transfer function were applied in the EM3DR program, which uses Fourier–Bessel routines to compute 3D reconstructions (Crowther, 1971). The resolution limit for each of the two final 3D reconstructions was estimated by subdividing the images within a data set into two roughly equal sets from which ‘even’ and ‘odd’ reconstructions and then structure factors were computed, and noting the spatial frequency at which the Fourier shell correlation coefficient comparing the ‘even’ and ‘odd’ data drops below a 0.5 threshold. On this basis, the resolution limits of the reconstructions of the RRV₂₁₈ and RRV₂₁₈/HS complex were determined to be 22 \AA and 24 \AA , respectively. For difference map analysis, the reconstructions of RRV₂₁₈ and of the RRV₂₁₈/HS complex were both computed to 24 \AA resolution and the maps were scaled in two ways. The pixel sizes in the two reconstructions were first adjusted to minimize differences in the outer leaflets of the viral membranes. Then, all density values in one of the maps were multiplied by a fixed factor and a constant was added in order to minimize differences within a defined radial region in each of the two maps. The precise selection of radii had minimal influence on the final results and their interpretation. In this study, we used density spanning (a) just glycoprotein shell ($r_1 = 257 \text{ \AA}$ to $r_2 = 353 \text{ \AA}$); (b) the genome, capsid, and membrane ($r_1 = 0 \text{ \AA}$ to $r_2 = 257 \text{ \AA}$); (c) the genome and capsid ($r_1 = 0 \text{ \AA}$ to $r_2 = 200 \text{ \AA}$); and (d) just the genome ($r_1 = 0 \text{ \AA}$ to $r_2 = 164 \text{ \AA}$). Regardless of which of the above methods was used to scale the maps, the most

prominent difference densities always occurred at the same locations attributable to HS density. The difference map portrayed in Fig. 1E was computed with only the density values for the genome ($r_1 = 0 \text{ \AA}$ to $r_2 = 164 \text{ \AA}$) used for scaling.

Acknowledgments

We thank R. Ashmore and J. Folk for assistance with programming and M. Rossmann for many invaluable discussions and critical insights. We thank T. Smith for providing the Fab model used in Fig. 3. This work was supported in part by National Institutes of Health grants to T.S.B. (AI 45976 and GM 33050) and R.J.K. (GM 56279), by NSF shared instrumentation grant to T.S.B. (BIR911291) for the FEI CM200 FEG microscope, and by a Purdue reinvestment grant to the Purdue Structural Biology group.

References

- Baker, T.S., Cheng, R.H., 1996. A model-based approach for determining orientations of biological macromolecules imaged by cryoelectron microscopy. *J. Struct. Biol.* 116, 120–130.
- Baker, T.S., Olson, N.H., Fuller, S.D., 1999. Adding the third dimension to virus life cycles: three-dimensional reconstruction of icosahedral viruses from cryo-electron micrographs. *Microbiol. Mol. Biol. Rev.* 63 (4), 862–922.
- Bernard, K.A., Klimstra, W.B., Johnston, R.E., 2000. Mutations in the E2 glycoprotein of Venezuelan equine encephalitis virus confer heparan sulfate interaction, low morbidity, and rapid clearance from blood of mice. *Virology* 276 (1), 93–103.
- Burness, A.T., Pardoe, I., Faragher, S.G., Vрати, S., Dalgarno, L., 1988. Genetic stability of Ross River virus during epidemic spread in nonimmune humans. *Virology* 167 (2), 639–643.
- Byrnes, A.P., Griffin, D.E., 1998. Binding of Sindbis virus to cell surface heparan sulfate. *J. Virol.* 72 (9), 7349–7356.
- Caspar, D.L.D., Klug, A., 1962. Physical principles in the construction of regular viruses. *Cold Spring Harbor Symp. Quant. Biol.* 27, 1–24.
- Chen, Y., Maguire, T., Hileman, R.E., Fromm, J.R., Esko, J.D., Linhardt, R.J., Marks, R.M., 1997. Dengue virus infectivity depends on envelope protein binding to target cell heparan sulfate. *Nat. Med.* 3 (8), 866–871.
- Cheng, R.H., Kuhn, R.J., Olson, N.H., Rossmann, M.G., Choi, H.-K., Smith, T.J., Baker, T.S., 1995. Nucleocapsid and glycoprotein organization in an enveloped virus. *Cell* 80, 621–630.
- Choi, H.-K., Tong, L., Minor, W., Dumas, P., Boege, U., Rossmann, M.G., Wengler, G., 1991. Structure of Sindbis virus core protein reveals a chymotrypsin-like serine proteinase and the organization of the virion. *Nature* 354, 37–43.
- Crowther, R.A., 1971. Procedures for three-dimensional reconstruction of spherical viruses by Fourier synthesis from electron micrographs. *Philos. Trans. R. Soc. Lond.* 261, 221–230.
- Fry, E.E., Lea, S.M., Jackson, T., Newman, H.W.I., Elland, F.M., Blakemore, W.E., Abu-Ghazaleh, R., Samuel, A., King, A.M.Q., Stuart, D.I., 1999. The structure and function of a foot-and-mouth disease virus-oligosaccharide receptor complex. *EMBO J.* 18 (3), 543–554.
- Garoff, H., Frischauf, A.M., Simons, K., Lehrach, H., Delius, H., 1980. Nucleotide sequence of cDNA coding for Semliki Forest virus membrane glycoproteins. *Nature* 288 (5788), 236–241.
- Heil, M.L., Albee, A., Strauss, J.H., Kuhn, R.J., 2001. An amino acid substitution in the coding region of the E2 glycoprotein adapts Ross

- River virus to utilize heparan sulfate as an attachment moiety. *J. Virol.* 75 (14), 6303–6309.
- Jackson, T., Ellard, F.M., Ghazaleh, R.A., Brookes, S.M., Blakemore, W.E., Corteyn, A.H., Stuart, D.I., Newman, J.W., King, A.M., 1996. Efficient infection of cells in culture by type O foot-and-mouth disease virus requires binding to cell surface heparan sulfate. *J. Virol.* 70 (8), 5282–5287.
- Kerr, P.J., Weir, R.C., Dalgarno, L., 1993. Ross River virus variants selected during passage in chick embryo fibroblasts: serological, genetic, and biological changes. *Virology* 193 (1), 446–449.
- Klimstra, W.B., Ryman, K.D., Johnston, R.E., 1998. Adaptation of Sindbis virus to BHK cells selects for use of heparan sulfate as an attachment receptor. *J. Virol.* 72 (9), 7357–7366.
- Kong, Y., Zhang, X., Baker, T.S., Ma, J., 2004. A structural-informatics approach for tracing beta-sheets: building pseudo-C(alpha) traces for beta-strands in intermediate-resolution density maps. *J. Mol. Biol.* 339 (1), 117–130.
- Krusat, T., Streckert, H.J., 1997. Heparin-dependent attachment of respiratory syncytial virus (RSV) to host cells. *Arch. Virol.* 142 (6), 1247–1254.
- Lee, S., Owen, K.E., Choi, H.K., Lee, H., Lu, G., Wengler, G., Brown, D.T., Rossmann, M.G., Kuhn, R.J., 1996. Identification of a protein binding site on the surface of the alphavirus nucleocapsid and its implication in virus assembly. *Structure* 4 (5), 531–541.
- Lescar, J., Roussel, A., Wien, M.W., Navaza, J., Fuller, S.D., Wengler, G., Rey, F.A., 2001. The Fusion glycoprotein shell of Semliki Forest virus: an icosahedral assembly primed for fusogenic activation at endosomal pH. *Cell* 105 (1), 137–148.
- Lin, C.L., Chung, C.S., Heine, H.G., Chang, W., 2000. Vaccinia virus envelope H3L protein binds to cell surface heparan sulfate and is important for intracellular mature virion morphogenesis and virus infection in vitro and in vivo. *J. Virol.* 74 (7), 3353–3365.
- Mancini, E.J., Clarke, M., Gowen, B., Rutten, T., Fuller, S.D., 2000. Cryo-electron microscopy reveals the functional organization of an enveloped virus, Semliki Forest virus. *Mol. Cell* 5, 255–266.
- McKnight, K.L., Simpson, D.A., Lin, S.C., Knott, T.A., Polo, J.M., Pence, D.F., Johannsen, D.B., Heidner, H.W., Davis, N.L., Johnston, R.E., 1996. Deduced consensus sequence of Sindbis virus strain AR339: mutations contained in laboratory strains which affect cell culture and in vivo phenotypes. *J. Virol.* 70 (3), 1981–1989.
- Ohuchi, M., Ohuchi, R., Feldmann, A., Klenk, H.D., 1997. Regulation of receptor binding affinity of influenza virus hemagglutinin by its carbohydrate moiety. *J. Virol.* 71 (11), 8377–8384.
- Olson, N.H., Baker, T.S., Johnson, J.E., Hendry, D.A., 1990. The three-dimensional structure of frozen-hydrated Nudaurelia Capensis beta virus, a T = 4 insect virus. *J. Struct. Biol.* 105, 111–122.
- Paredes, A.M., Brown, D.T., Rothnagel, R., Chiu, W., Schoepp, R.J., Johnston, R.E., Prasad, B.V.V., 1993. Three-dimensional structure of a membrane-containing virus. *Proc. Natl. Acad. Sci. U.S.A.* 90, 9095–9099.
- Paredes, A.M., Heidner, H., Thuman-Commike, P., Venkataram Prasad, B.V., Johnston, R.E., Chiu, W., 1998. Structural localization of the E3 glycoprotein in attenuated sindbis virus mutants. *J. Virol.* 72 (2), 1534–1541.
- Paredes, A., Alwell-Warda, K., Weaver, S.C., Chiu, W., Watowich, S.J., 2003. Structure of isolated nucleocapsids from Venezuelan equine encephalitis virus and implications for assembly and disassembly of enveloped virus. *J. Virol.* 77 (1), 659–664.
- Patel, M., Yanagishita, M., Roderiquez, G., Bou-Habib, D.C., Oravec, T., Hascall, V.C., Norcross, M.A., 1993. Cell-surface heparan sulfate proteoglycan mediates HIV-1 infection of T-cell lines. *AIDS Res. Hum. Retroviruses* 9 (2), 167–174.
- Pletnev, S.V., Zhang, W., Mukhopadhyay, S., Fisher, B.R., Hernandez, R., Brown, D.T., Baker, T.S., Rossmann, M.G., Kuhn, R.J., 2001. Locations of carbohydrate sites on Sindbis virus glycoproteins show that E1 forms an icosahedral scaffold. *Cell* 195, 127–136.
- Skehel, J.J., Stevens, D.J., Daniels, R.S., Douglas, A.R., Knossow, M., Wilson, I.A., Wiley, D.C., 1984. A carbohydrate side chain on hemagglutinins of Hong Kong influenza viruses inhibits recognition by a monoclonal antibody. *Proc. Natl. Acad. Sci. U.S.A.* 81 (6), 1779–1783.
- Smith, T.J., Cheng, R.H., Olson, N.H., Peterson, P., Chase, E., Kuhn, R.J., Baker, T.S., 1995. Putative receptor binding sites on enveloped viruses as visualized by cryo-electron microscopy. *Proc. Natl. Acad. Sci. U.S.A.* 92, 10648–10652.
- Strauss, J.H., Strauss, E.G., 1994. The alphaviruses: gene expression, replication, and evolution. *Microbiol. Rev.* 58 (3), 491–562.
- Strauss, E.G., Stec, D.S., Schmaljohn, A.L., Strauss, J.H., 1991. Identification of antigenically important domains in the glycoproteins of Sindbis virus by analysis of antibody escape variants. *J. Virol.* 65 (9), 4654–4664.
- Strauss, J.H., Rumenapf, T., Weir, R.C., Kuhn, R.J., Wang, K.-S., Strauss, E.G., 1994. Cellular receptors for alphaviruses. In: Wimmer, E. (Ed.), *Cellular Receptors for Animal Viruses*. Cold Spring Harbor Laboratory Press, Plainview, NY, pp. 141–163.
- Summerford, C., Samulski, R.J., 1998. Membrane-associated heparan sulfate proteoglycan is a receptor for adeno-associated virus type 2 virions. *J. Virol.* 72 (2), 1438–1445.
- Taylor, R.M., Hurlbut, H.S., Work, T.H., Kingston, J.R., Frothingham, T.E., 1955. Sindbis virus: a newly recognized arthropodtransmitted virus. *Am. J. Trop. Med. Hyg.* 4 (5), 844–862.
- Ubol, S., Griffin, D.E., 1991. Identification of a putative alphavirus receptor on mouse Alphaviruses replicate in a wide variety of cells in vitro. *J. Virol.* 65 (12), 6913–6921.
- Vrati, S., Faragher, S.G., Weir, R.C., Dalgarno, L., 1986. Ross River virus mutant with a deletion in the E2 gene: properties of the virion, virus-specific macromolecule synthesis, and attenuation of virulence for mice. *Virology* 151 (2), 222–232.
- Vrati, S., Fernon, C.A., Dalgarno, L., Weir, R.C., 1988. Location of a major antigenic site involved in Ross River virus neutralization. *Virology* 162 (2), 346–353.
- WuDunn, D., Spear, P.G., 1989. Initial interaction of herpes simplex virus with cells is binding to heparan sulfate. *J. Virol.* 63 (1), 52–58.
- Zhang, W., Fisher, B.R., Olson, N.H., Strauss, J.H., Kuhn, R.J., Baker, T.S., 2002a. Aura virus structure suggests that the T = 4 organization is a fundamental property of viral structural proteins. *J. Virol.* 76, 7239–7246.
- Zhang, W., Mukhopadhyay, S., Pletnev, S.V., Baker, T.S., Kuhn, R.J., Rossmann, M., 2002b. Placement of the structural proteins in Sindbis virus. *J. Virol.* 76 (22), 11645–11658.
- Zhang, X., Walker, S.B., Chipman, P.R., Nibert, M.L., Baker, T.S., 2003. Reovirus polymerase lambda 3 localized by cryo-electron microscopy of virions at a resolution of 7.6 Å. *Nat. Struct. Biol.* 10 (12), 1011–1018.